HHS Public Access

Author manuscript

Nanotoxicology. Author manuscript; available in PMC 2024 February 16.

Published in final edited form as:

Nanotoxicology. 2023 December ; 17(10): 669–686. doi:10.1080/17435390.2023.2297048.

Lung toxicity, deposition, and clearance of thermal spray coating particles with different metal profiles after inhalation in rats

James M. Antonini[a], **Vamsi Kodali**[a], **Terence G. Meighan**[a], **Walter McKinney**[a], **Jared L. Cumpston**[a], **Howard D. Leonard**[a], **James B. Cumpston**[a], **Sherri Friend**[a], **Stephen S. Leonard**[a], **Ronnee Andrews**[a], **Patti C. Zeidler-Erdely**[a], **Aaron Erdely**[a], **Eun Gyung Lee**[b], **Aliakbar A. Afshari**[a]

[a]Health Effects Laboratory Division, National Institute for Occupational Safety and Health, Morgantown, WV, USA

[b]Respiratory Health Division, National Institute for Occupational Safety and Health, Morgantown, WV, USA

Abstract

Thermal spray coating is a process in which molten metal is sprayed onto a surface. Little is known about the health effects associated with these aerosols. Sprague-Dawley rats were exposed to aerosols (25 mg/m^3 × 4 hr/d × 4 d) generated during thermal spray coating using different consumables [i.e. stainless-steel wire (PMET731), Ni-based wire (PMET885), Zn-based wire (PMET540)]. Control animals received air. Bronchoalveolar lavage was performed at 4 and 30 d post-exposure to assess lung toxicity. The particles were chain-like agglomerates and similar in size (310–378 nm). Inhalation of PMET885 aerosol caused a significant increase in lung injury and inflammation at both time points. Inhalation of PMET540 aerosol caused a slight but significant increase in lung toxicity at 4 but not 30 d. Exposure to PMET731 aerosol had no effect on lung toxicity. Overall, the lung responses were in the order: PMET885>>PMET540 > PMT731. Following a shorter exposure (25 mg/m^3 × 4 h/d × 1d), lung burdens of metals from the different aerosols were determined by ICP-AES at 0, 1, 4 and 30 d post-exposure. Zn was cleared from the lungs at the fastest rate with complete clearance by 4 d post-exposure. Ni, Cr, and Mn had similar rates of clearance as nearly half of the deposited metal was cleared by 4 d. A small but significant percentage of each of these metals persisted in the lungs at 30 d. The pulmonary clearance of Fe was difficult to assess because of inherently high levels of Fe in control lungs.

CONTACT James Antonini, JGA6@cdc.gov, Health Effects Laboratory Division, Centers for Disease Control & Prevention, National Institute for Occupational Safety and Health, 1000 Frederick Lane (Mailstop 2015), Morgantown, WV 26508, USA.

Disclosure statement

No potential conflict of interest was reported by the author(s).

Disclaimer

The findings and conclusions in this report are those of the authors and do not necessarily represent the official position of the National Institute for Occupational Safety and Health, Centers for Disease Control and Prevention. Mention of brand name does not constitute product endorsement.

Keywords

Thermal spray coating; metals; particulates; inhalation; lung toxicity

1. Introduction

Thermal spray coating applies a metal coating product that is melted by very high temperatures (ranging up to 16,000 °C) and then deposited under pressure onto different surface substrates (Oerlikon Metco 2016). Thermal spray processes are simple to perform, economical, and have beneficial coating attributes for many industries, such as aerospace, gas and energy, automotive, steel, medical, electronics, salvage and restoration (ASM Thermal Spray Society 2023). Applications include coatings for wear prevention and sealing, thermal insulation, oxidation and corrosion resistance, restoration and decoration, and fabrication of free-standing components and spray-formed parts. Occupational exposure to aerosols generated during thermal spray coating is an emerging hazard as the global market for specific thermal spray applications is predicted to be 15.41 billion dollars by 2030 (Grand View Research 2023) and the number of workers in coating and spraying continues to grow (U.S. Bureau of Labor Statistics 2022).

An aerosol containing a mixture of metals [e.g. nickel (Ni), zinc (Zn), chromium (Cr), manganese (Mn), iron (Fe)] is produced during the thermal spray coating process that may pose an adverse health risk to the operator, who often performs the process without proper respiratory protection, as well as to other workers in the vicinity of the operation who are not using any respiratory protection at all. The produced particulates are in the fine and ultrafine size ranges (Afshari et al. 2022; Bémer et al. 2010; Kodali et al. 2022). Workplace exposure levels of total and specific metals generated during thermal spray coating have been reported to be excessively high, oftentimes exceeding local workplace exposure limits. Different industrial hygiene groups have measured hexavalent chromium exposures ‘to be greater than 500 μg/m^3 in an open air work area that approached 100 times the OSHA permissible exposure limit of 5 μg/m^3’ (A. Siert, Xcel Energy, February, 2017; personal correspondence) and ‘to be 20–40 times higher than the permissible exposure limit for a 12-hr work shift’ (L.P. Dutton, Work Environment Associates, June, 2008; personal correspondence). In addition, Huang, Li, and Li (2016) measured a time-weighted average concentration of 34.2 mg/m^3 that had a peak total dust concentration of 140 mg/m^3 during spray coating in a Chinese workshop. These concentrations far exceeded established workplace limits by 4 and 8 times, respectively. Bémer et al. (2010) also observed extremely high emission rates for electric arc thermal spray coating with concentrations measured as high as 10^8 particles/cm^3 inside a well-ventilated cabin.

Further evidence of exposures has been illustrated through biomonitoring, for example, Chadwick, Wilson, and White (1997) found that urinary chromium concentrations were high in workers performing electric arc thermal spray coating. Unfortunately, detailed information about the possible health effects associated with exposure to thermal spray coating aerosols is lacking (Antonini et al. 2021). Toxicology studies are needed to characterize the formed aerosols as well as to examine their potential toxicity in a

controlled laboratory setting. The goal was to chemically and physically characterize aerosols generated during electric arc thermal spray coating using three consumable wires with distinctly different metal profiles: (1) Ni-based PMET885, (2) Zn-based PMET540, and (3) stainless steel PMET731. Male Sprague-Dawley rats were exposed by inhalation of 25 mg/m^3 for 4 hr/d × 4 d of aerosols generated during electric arc thermal spray coating using the three different wires. Lung injury and inflammation were examined at 4 and 30 d after the final exposure. In addition, the lung deposition and clearance of the total and specific metals after exposure were determined at multiple time points after a single exposure to the different aerosols.

2. Materials AND METHODS

2.1. Thermal spray coating aerosol generation and exposure system

A computer-controlled thermal spray coating generator and inhalation exposure system was constructed to perform animal studies to mimic workplace exposures in a laboratory as previously described (Afshari et al. 2022; Kodali et al. 2022). Rats were exposed by inhalation of aerosols (target concentration: 25 mg/m^3 × 4 hr/d × 4 d) generated from electric arc wire thermal spray coating (AT-400 Wire Arc Spray System; Thermach, Inc., Medina, WI) using different consumable wires at specified operational spray coating settings (Polymet Corporation, West Chester, OH), including a stainless-steel wire (PMET731; settings of 60 psi, 30 V, 200 A), a Ni-based wire (PMET885; settings of 60 psi, 30 V, 250 A), and a Zn-based wire (PMET540; settings of 60 psi, 23 V, 200 A). Control animals were exposed to filtered air in a separate but identical exposure chamber. The different thermal spray coating aerosols were generated in a closed spray booth and piped into an animal exposure chamber where they were collected and characterized.

The thermal spray coating exposure system was divided into two separated areas (Figure 1): (A) an enclosed room where the spray coating occurred that contained a compressed air tank, thermal spray machine with wire holder and feeder unit; (B) the animal exposure chamber equipped with different particle characterization, chamber condition devices, and air flow controllers.

Within the spray booth, different consumable thermal spray coating metal wires were fed independently into the spray gun. The wires were then charged, and an arc was generated between them. The heat from the arc melted the incoming wires, and the molten metal particles were suspended in a jet of air from the gun. The suspended molten metal particles were deposited onto the metal feedstock pipe that can be rotated during the 4-hr exposure time. The spray gun was controlled by a computer program and was fired at selected intervals to produce a target concentration of 25 mg/m^3 in the exposure chamber. The system allowed for the simultaneous exposure of a maximum of 12 animals.

After leaving the booth, the aerosol was diluted by mixing with air and passed through a cyclone (URG-2000-30EP, URG Corp, Chapel Hill NC) to further remove large particles. The upper diameter limit of the cyclone was 6 mm at a flow of 31 L/min. The flow into the cyclone was maintained at 31 L/min, by using a mass flow controller. Large particles

were removed so that the animals would receive predominantly the respirable portion of the particles (<6 μm).

The mass concentration in the chamber was monitored by a real-time aerosol monitor (DataRAM, MIE, Inc., Bedford, MA). The sensors and measurement devices were managed and controlled through a custom computer software program written in LabVIEW (National Instruments Corporation, Austin, TX). To maintain a constant particle concentration in the exposure chamber, the software would adjust the amount of dilution air that made up the 31 L/min entering the exposure chamber. Particle mass concentrations inside the animal chamber were determined by collecting airborne particles with two, 47-mm closed-face cassettes loaded with polytetrafluoroethylene filters followed by gravimetric analyses.

Multiple ports were located on the top of the chamber and used to measure chamber pressure and to collect additional particle samples for size distribution, chemical composition, and electron microscopy analyses. The air change range is approximately 8–10 changes/min. The air pressure and temperature and relative humidity inside the chamber were continually measured during the exposure period (Vaisala Temperature-Humidity Probe, model# HMP60; Woburn, MA). The levels of generated carbon dioxide (Vaisala CO_2 Probe, model# GMP252; Woburn, MA) were continuously monitored in the chamber during animal exposures and maintained below 5000 ppm.

2.2. Thermal spray coating aerosol characterization

2.2.1. Particle size and morphology—Size distribution of the thermal spray coating aerosols inside the exposure chamber was determined using a Micro-Orifice Uniform Deposit Impactor (MOUDI; MSP Model 110, MSP Corporation, Shoreview, MN). The MOUDI separated the particles into 11 size ranges (stages), with particles within each range being collected on an aluminum foil filter placed on the applicable stage. The total size range considered was 0056 – 18 μm. The mass median aerodynamic diameter (MMAD) and geometric standard deviation (GSD) were determined from the gravimetric measurements of the particles deposited on the foil filters for the different stages. For imagining purposes, generated particles were collected using 47-mm cassettes loaded with polycarbonate filters (0.2 μm pore size; Whatman, Clinton, PA). Particle morphology was assessed using a Hitachi S4800 field emission scanning electron microscope (SEM; Hitachi High-Tech America, Boston, MA).

2.2.2. Metal composition—Particle samples were collected inside the exposure chamber onto 5 μm pore size polyvinyl chloride membrane filters (SKC, inc., Eighty Four, PA) in 37-mm cassettes during thermal spray coating using the different consumable wires. The collected samples were analyzed for metal components using inductively coupled plasma-atomic emission spectroscopy (ICP-AES) according to NIOSH Method 7303 modified for hot block/HCl/HNO_3 digestion (NIOSH 1994). Blank filters also were analyzed for control purposes. The LODs for the method for the measured metals were: Cr (0.061 μg/sample), Fe (0.73 μg/sample), Mn (0.019 μg/sample), Ni (0.022 μg/sample), and Zn (0.45 μg/sample). The LOQs for the method for the measured metals were: Cr (0.193

μg/sample), Fe (2.32 μg/sample), Mn (0.0619 μg/sample), Ni (0.0698 μg/sample), and Zn (1.43 μg/sample).

2.2.3. Electron paramagnetic resonance—To detect and measure short-lived free radical intermediates, electron paramagnetic resonance (EPR) spin-trapping was used. To assess whether the thermal spray coating particle suspensions could produce hydroxyl radicals, they were exposed to H_2O_2 through a Fenton-like reaction. Final concentrations were 100 mM of the spin-trap DMPO (5,5′-dimethyl-pyrroline N-oxide, Sigma-Aldrich, St. Louis, MO), 5 mg/ml of the thermal spray coating particle or potassium dichromate [2 mM; Cr (VI) positive control], and 1 mM H_2O_2 suspended in phosphate buffered saline (PBS) and mixed in the order listed. All reagents were combined for 3 min at room temperature and then filtered to halt the reaction and remove any metal particles. The sample was then transferred to a quartz flat cell for EPR measurement in a Bruker EMX spectrometer (Bruker Instruments Inc., Billerica, MA). For each sample, the instrument ran 3 scans with a 41 sec scan time, a receiver gain of 1.0×10^4, a 40 msec time constant, 1.0 G modulation amplitude, 63.4 mW power, 9.751 frequency, and 3515 G magnetic field center. Samples were run in independent experiments ($n = 3$). Sample data were attained and processed as previously described (Leonard et al. 2004; Stefaniak et al. 2009). Briefly, signal intensity (peak height) from the 1:2:2:1 spectrum (characteristic for hydroxy radical) was used to measure the relative proportion of the short-lived radicals trapped.

2.3. Animals

Male Sprague-Dawley rats (Hilltop Lab Animals, Scottdale, PA) were used and weighed 250–300 g upon arrival. They were free of viral pathogens, parasites, mycoplasmas, *Helicobacter*, and CAR bacillus and were provided HEPA-filtered air, irradiated Teklad 2918 diet, and tap water *ad libitum*. The rats were acclimated for one week after arrival. All animal procedures used were reviewed by the Centers for Disease Control and Prevention (CDC), Morgantown NIOSH Animal Care and Use Committee (ACUC). The animal facilities are specific pathogen-free and environmentally controlled. The program and the facility are accredited by the AAALAC International (Frederick, MD).

2.4. Lung toxicity study

2.4.1. Inhalation exposure—The rats were exposed in a whole body chamber to the respirable portion (<6 μm) of aerosols (target concentration: 25 mg/m^3 × 4 hr/d × 4 d) generated from electric arc wire thermal spray coating using (1) a stainless-steel consumable wire (PMET731), (2) a Ni-based consumable wire (PMET885), and (3) a Zn-based consumable wire (PMET540). Control animals were exposed to filtered air. The system was designed to expose 12 rats/treatment group at a time (one rack of 12 animals for the test material and one rack of 12 animals in a separate chamber for the air controls). Exposed animals were harvested at 4 and 30 d after the last exposure. Animal body weights were measured during the exposure period and throughout the 30 d post-exposure period. For all exposures, $n = 6$ animals/treatment group within a time point.

The aerosols were generated in a closed spray booth and piped to the exposure chamber. The target concentration of 25 mg/m^3 was chosen as it was in the range (12–140 mg/m^3)

measured in workplaces where thermal spray coating occurred (Darut et al. 2021; Huang, Li, and Li 2016; Petsas et al. 2007). It is also comparable to concentration (15–40 mg/m^3) used in similar animal inhalation toxicology studies of other metal particles, such as welding fumes (Antonini et al. 2007; 2017; 2020). The actual daily mean (± standard deviation) exposure chamber concentrations for the 4-d exposures were as follows: PMET731 (21.5 ± 8.1 mg/m^3), PMET885 (24.6 ± 5.8 mg/m^3), and PMET540 (24.9 ± 3.1 mg/m^3).

2.4.2. Bronchoalveolar lavage—At 4 and 30 d after the final inhalation exposure, bronchoalveolar lavage (BAL) was performed to assess lung injury and inflammation. Animals were euthanized with an overdose of a pentobarbital-based euthanasia solution (100–300 mg/kg, IP; Fatal-Plus Solution, Vortech Pharmaceutical, Inc., Dearborn, MI) and then exsanguinated by severing the abdominal aorta. The right lung was first lavaged with a 1 ml/100 g body weight aliquot of calcium- and magnesium-free PBS, pH 7.4. The first fraction of recovered BAL fluid (BALF) was centrifuged at 500 × g for 10 min, and the resultant cell-free supernatant was saved for lung cell damage analysis. The right lung was further lavaged with 6-ml aliquots of PBS until 30 ml were collected. These samples also were centrifuged for 10 min at 500 × g and the cell-free BALF fraction was discarded. The cell pellets from all washes for each rat were combined, re-suspended in 1 ml of PBS buffer, counted, and differentiated.

2.4.3. Assessment of lung injury and inflammation—Lactate dehydrogenase (LDH) was measured in the first fraction of the cell-free supernatant recovered from the BALF as a general marker for lung toxicity. LDH activity was determined by measuring the oxidation of lactate to pyruvate coupled with the formation of NADH at 340 nm. Measurements were taken with a COBAS MIRA auto-analyzer (Roche Diagnostic Systems, Montclair, NJ). For the determination of lung inflammation, total cell numbers recovered by BAL from the right lung were determined using a Coulter Multisizer II and AccuComp software (Coulter Electronics, Hialeah, FL). Cell suspensions (5 × 10^4 cells) were spun using a Cytospin 3 centrifuge (Shandon Life Sciences International, Cheshire, England) for 5 min at 800 rpm onto a slide. Cells (200/rat) were identified after labeling with Leukostat stain (Fisher Scientific, Pittsburgh, PA) as monocytes/alveolar macrophages (AM), neutrophils, and eosinophils (EOS).

2.5. Lung deposition and clearance study

2.5.1. Inhalation exposure—The rats were exposed in a whole body chamber to the respirable portion of aerosols (target concentration: 25 mg/m^3 × 4 hr/d × 1 d) generated from electric arc wire thermal spray coating using (1) a stainless-steel consumable wire (PMET731; settings of 60 psi, 30 V, 200 A), (2) a Ni-based consumable wire (PMET885; settings of 60 psi, 30 V, 250 A), and (3) a Zn-based consumable wire (PMET540; settings of 60 psi, 23 V, 200 A). Control animals were exposed to filtered air. Rats (n = 6/group) were immediately harvested following the exposure (0 d), and at 1, 4, and 30 d post-exposure. As opposed to the lung toxicity study (section 2.4), the inhalation exposures were performed for 1 d instead of 4 d. This was done to reduce the complications of sequential deposition and clearance during an extended exposure. Due to space limitations, two exposures were performed for each of the three consumables. Exposure for the first two time points (days 0

and 1) were performed on one day, and the exposure for the second two time points (days 4 and 30) were performed on the next day. The actual daily 4-hr time-weighted average exposure chamber concentrations were as follows: PMET731 (exposure 1: 19.3 mg/m^3, exposure 2: 23.9 mg/m^3), PMET885 (exposure 1: 22.1 mg/m^3, exposure 2: 24.3 mg/m^3), and PMET540 (exposure 1: 19.7 mg/m^3, exposure 2: 23.6 mg/m^3). It is important to note that there is some variation in chamber exposure concentration during the course of the daily 4-hr exposures. When the mean exposure concentrations for the 4-hr exposures for the two days were compared for each specific thermal spray test material, they were not significantly different. For all exposures for the clearance studies, $n = 6$ animals/treatment group within a time point.

2.5.2. Lung deposition and clearance of metals—To assess the pulmonary clearance of deposited thermal spray coating particles, the metal content present in the lungs was measured on days 0, 1, 4 and 30 after the single 4-hr exposure. The concentration of specific metals deposited in the lungs at each time point was determined by ICP-AES according to NIOSH method 8200 (NIOSH 2018), modified for closed-vessel microwave digestion. Non-lavaged whole lungs were collected from each animal, weighed, and lyophilized. The lung tissue samples were transferred to vessels for digestion. The samples were treated with 10 ml of concentrated nitric acid and 2 ml of deionized water, capped, and temperature ramped to 180 °C and held for 10 min. The sample residues were diluted to 45 mL (22% nitric acid final concentration) and then analyzed for trace metals by ICP-AES.

2.6. Statistics

Statistical analyses were performed using JMP version 13 (SAS Institute, Cary, NC). All treatments were compared for statistical significance using factorial analysis of variance (ANOVA), either one- or two-way depending on the experimental design. ANOVA was followed by multiple comparison post hoc test for pairwise comparison using Tukey's or Fishers Least Significant Difference (LSD). Differences were considered statistically significant at $p < 0.05$.

3. Results

3.1. Aerosol characterization

ICP-AES measurement showed that the aerosols generated during thermal spray coating using the PMET885 and PMET540 wire were composed of predominately one metal each, Ni (96.9%) and Zn (99.4%), respectively (Table 1). The aerosol generated using the stainless steel wire (PMET731) was primarily composed of three metals – Fe (66.3%), Cr (26.2%), and Mn (1.02%). Representative size distribution graphs for the different thermal spray coating aerosols are shown in Figure 2. The three generated aerosols had similar MMADs (ranging from 310 to 378 nm) and geometric standard deviations (ranging from 1.89 to 1.94). SEM analysis indicated that the generated particles from thermal spray coating using different wires were arranged as agglomerated chains of ultrafine-size primary particles (Figure 3). Large, more spherical particles were also observed. EPR analysis indicated that each of the different thermal spray coating aerosols had some surface reactivity with PMET540 and PMET731 being the most reactive (Figure 4, inset). Each of the thermal

spray coating aerosol samples were significantly less reactive than the Cr(VI) positive control (Figure 4).

3.2. Body weight, lung injury and inflammation

As an assessment of general health, animal body weight was measured after the start of the exposure to the different thermal spray coating aerosols at different time points after the exposure started (Figure 5). For this index, day 0 is considered the start of the exposure and day 34 is considered the end time point or 30 d after the final exposure. Inhalation of the stainless steel PMET731 and Zn-based PMET540 aerosols had no effect on body weight gain at any time point during and after exposure as compared to air control (Figure 5A & C). However, inhalation of the Ni-based PMET885 aerosol caused a significant loss in body weight as soon as 4 d after the exposure had started with the weight loss continuing up to 7 d (Figure 5B). Although this group began to gain weight again, the animals exposed to the Ni-based PMET885 aerosol weighed significantly less than the air control at each time point assessed (Figure 5B&D).

In the measurement of lung injury, LDH was measured in the acellular BALF at 4 and 30 d after inhalation exposure to the different thermal spray coating aerosols (Figure 6). Pulmonary exposure to aerosols using a stainless steel wire (PMET731) had no effect on BALF LDH when compared to air control at either time point examined (Figure 6A). BALF LDH was significantly increased compared to air control at both 4 and 30 d after exposure to the Ni-based (PMET885) thermal spray coating aerosol (Figure 6B). Exposure to aerosols generated using a Zn-based PMET540 wire had a significant, but transient, increase in lung injury as BALF LDH was elevated at 4 d but returned to control level by 30 d (Figure 6C). When comparing the different thermal spray coating aerosols as % air control at the two time points, the Ni-based PMET885 aerosol was substantially more toxic to the lungs compared to the other two aerosols (Figure 6D).

In the assessment of lung inflammation, the total number of BAL cells recovered from the lungs were counted at 4 and 30 d after inhalation exposure to different thermal spray coating aerosols (Figure 7). Inhalation exposure to aerosols using a stainless steel wire (PMET731) had no effect on total BAL cells recovered when compared to air control at both time points (Figure 7A). The total number of BAL cells recovered from the lungs were significantly increased compared to air control at both 4 and 30 d after exposure to the Ni-based (PMET885) thermal spray coating aerosol (Figure 7B). Interestingly, total cells were increased in the PMET885 group at 30 d post-exposure compared to 4 d. As observed with BALF LDH, pulmonary exposure to aerosols generated using a Zn-based PMET540 wire had a significant, but transient, increase in lung inflammation as total BAL cells were elevated at 4 d but returned to control level by 30 d (Figure 7C). When comparing lung inflammation among the different thermal spray coating aerosols as % air control, the Ni-based PMET885 was significantly more inflammatory to the lungs compared to the other aerosols at both time points (Figure 7D).

In the assessment of the specific lung cell types recovered after exposure to the different thermal spray coating aerosols (Table 2), the stainless steel PMET731 aerosol had no significant effect on the number of AMs, neutrophils, and EOS recovered by BAL compared

to air control at 4 and 30 d. However, BAL AMs, neutrophils, and EOS all were significantly elevated after inhalation of aerosols generated using the Ni-based PMET885 wire compared to air control at 4 and 30 d. Interestingly, the lung inflammatory response appeared to be progressing as both AMs and neutrophils were significantly elevated at 30 d compared to 4 d after exposure to the Ni-based PMET885 aerosol. BAL AMs were significantly increased at 4 d after exposure to the Zn-based PMET540 aerosol compared to air control. Also, as seen in Figure 8B, the BAL fluid had an irregular basophilic staining that is commonly see in alveolar lipoproteinosis. Alveolar lipoproteinosis tends to occur after necrosis of alveolar type I cells (consistent with the LDH increase), with replication of alveolar type II cells which are often hypertrophied.

Representative cytospin micrographs indicated that most of the cells recovered from BAL after exposure to each of the thermal spray coating aerosols were AMs (Figures 8 and 9). The presence of significant numbers of foamy cells (F), multinucleated giant cells (M), EOS (asterisks), and neutrophils (arrows) were observed at both 4 and 30 d after exposure to the Ni-based PMET885 aerosol (Figures 8B and 9B). The presence of neutrophils (arrows) were observed among the collected BAL cells after exposure to the Zn-based PMET540 aerosol at 4 and 30 d after exposure (Figures 8C and 9C). Neutrophils were not observed from air controls at either time point.

3.3. Lung deposition and clearance of metals

In the assessment of the pulmonary deposition and clearance of metals after inhalation of the thermal spray coating aerosols, the concentrations of individual metals were measured in the lungs at different time points after exposure to the different thermal spray coating aerosols and filtered air (Table 3). Before metal clearance was analyzed, the concentrations of the specific metals (Ni, Zn, Cr, Fe, and Mn) in the lungs of the air control samples were subtracted from the corresponding metal concentrations measured in the lungs after exposure to the different thermal spray aerosols (Table 3, last column). For some of the metals, it appeared that the target metals (Ni, Zn, Fe, Cr, and Mn) present in the different thermal spray coating aerosols demonstrated a two-compartment model of clearance as seen with many metal particles after inhalation. There was an initial soluble phase (fast clearance-a combination of dissolution and mucociliary-assisted clearance) in which a significant portion of the metals were cleared by 4 d after exposure as well as a slower clearance phase where the soluble portion of the metals had been removed, leaving the insoluble secondary particles to persist for a longer period in the lungs. The % metal remaining in the lungs over time after deposition at day 0 was compared for the different metals (Table 3, last column). The deposited Zn after inhalation of the PMET540 aerosol was cleared from the lungs at the fastest rate, with a significant amount (approximately 74%) being cleared by 1 d and most of the rest cleared by 4 d post-exposure. Ni, Cr, and Mn had similar rates of clearance as nearly half of the deposited metal was cleared by 4 d. A small but significant percentage of each of these metals (Ni: 21.2%; Cr: 23.2%; Mn 11.8%) persisted in the lungs at 30 d after exposure. The clearance of Fe was difficult to assess, complicated by the normally high levels of Fe in the lungs of the control animals (Table 3, 2nd column).

4. Discussion

Information about the health effects associated with exposure to aerosols generated during thermal spray operations is lacking. There is limited information about the physical (e.g. particle morphology and size) and chemical (e.g. metal composition, surface chemistry) properties of aerosols formed during various thermal spray coating processes. Because thermal spray coating is a fast-growing and emerging industry and the aerosols generated during these processes have not been fully investigated, the goal of the current study was to characterize and assess the potential pulmonary toxicity of aerosols formed during different types of thermal spray coating processes in a laboratory and whole-animal model. The proposed study was initiated because of concerns raised by workers and industrial hygiene groups in various metal industries where exposures to specific metals were extremely high and exceeded workplace exposure limits (Antonini et al. 2021).

There are two basic methods used to generate thermal spray coating- (1) electric energy and (2) combustion (Antonini et al. 2021). The initial goal of the project was to assess the lung toxicity of aerosols generated using electric energy thermal spray coating, a common and popular process used in U.S. industries. Our group has constructed and tested an electric arc wire thermal spray coating aerosol generator and animal inhalation exposure system (Afshari et al. 2022). In this current study, we examined the physio-chemical properties and lung toxicity of the aerosols formed during electric arc thermal spray coating with three chemically distinct consumable wires, using a well-controlled laboratory model that mimicked workplace exposure conditions.

The morphology of the generated thermal spray coating particles in the current study, regardless of metal composition, appeared nearly identical as observed by SEM analysis to welding fume, a well-characterized metal particle generated in the workplace. Like welding fume formation, the metal vapors produced during thermal spray coating are transformed into ultrafine-size primary particles (<100 nm) that coalescence and grow into long, chain-like agglomerates due to the extremely high temperatures and turbulent conditions of the process. Ultrafine-size primary particles as well as fine- and micron-size agglomerates have been observed by others to be formed during different thermal spray coating processes when using consumables of various metal profiles (Bemer et al. 2010; Huang, Li, and Li 2016; Salmatonidis et al. 2019). It also has been reported that approximately 90% of these formed particles were in the ultrafine size range (Bemer et al. 2010; Salmatonidis et al. 2019). MOUDI measurements of the three different types of thermal spray coating particles generated in the current study observed similar particle sizes with MMADs that ranged from 310 to 378 nm. The metal composition of the formed thermal spray coating aerosols in the current study was nearly identical to the metal profile of the wire (according to the manufacturer’s specification) that was consumed in the process.

Acellular particle reactivity and the oxidative stress potential of the different thermal spray coating aerosol were assessed by their ability to produce Fenton-like, short-lived free radical intermediates using EPR. It was observed that each of the different thermal spray coating aerosols evaluated in the current study produced free radical intermediates and had some surface reactivity. Interestingly, the PMET540 and PMET731 particle samples were more

reactive than the Ni-based PMET885 sample. Each of the thermal spray coating aerosol samples were significantly less reactive than the Cr(VI) positive control. This finding agreed with what was observed in the EPR analysis of another stainless steel (PMET720) thermal spray coating particle sample (Kodali et al. 2022). The average signal intensity of the PMET720 particle sample was significantly less than what was observed for the Cr(VI) positive control and two well-characterized stainless steel welding fume samples. In a previous study, a Ni-based welding fume did not enhance intracellular oxidant production in lung macrophages, whereas a mild steel and stainless steel welding fume did (Antonini et al. 2014), agreeing with the observation of the current study.

Overall, acellular reactivity did not correlate with toxicity outcomes. Acellular surface reactivity of a particulate was measured in the current study to correlate with pulmonary inflammation and toxicity. It was used as a metric to predict and group toxicity of different particulate materials (Bahl et al. 2020). Although there was significant increase in acellular surface reactivity by PMET540 and PMET731 compared to the PMET885 particulate, lung toxicity was substantially elevated after exposure to the PMET885 aerosol. There are multiple mechanisms in which particles may be toxic to cells. A number of *in vitro* studies are currently ongoing in the laboratory assessing intracellular oxidative stress and direct cytotoxicity of different lung cells as well as examining alterations in lung phagocyte activation and uptake after exposure to different thermal spray coating particle samples.

In the assessment of lung toxicity, the inhalation exposure (25 mg/m^3 × 4 hr/d × 4 d) to aerosols using the stainless steel wire (PMET731) had no effect on either BAL parameter of lung toxicity at the two time points examined. However, particles were easily observed in AMs at both 4 and 30 d after exposure to the PMET731 aerosol in the current study. The lack of inflammation or cytotoxicity as assessed by BAL parameters was unexpected as the PMET731 aerosol was composed of metals, specifically Cr, known to cause lung toxicity after exposure. Also, the PMET731 aerosol (66.3% Fe, 26.2% Cr, 1.02% Mn) was similar to stainless steel welding fume in terms of metal composition (57.2% Fe, 20.3% Cr, 13.8% Mn) and particle size and morphology. Previously, we have shown that animals exposed to the stainless steel welding fume (40 mg/m^3 × 3 hr/d × 3 d) displayed significant lung injury as soon as 1 d after exposure with both injury and inflammation persisting for weeks following the end of the post-exposure period (Antonini et al. 2007).

In a related study, we examined the lung response after inhalation (25 mg/m^3 × 4 hr/d × 9 d) to a different stainless steel (PMET720) thermal spray coating aerosol (Kodali et al. 2022). Although lung inflammation and injury were significantly elevated at 1 d after exposure to the PMET720 aerosol (82.2% Fe, 13.4% Cr, 2.37% Mn), the response was transient as both parameters of lung toxicity returned to control values by 7 d. The difference in the lung responses between the PMET731 aerosol of the current study with the PMET720 aerosol of the previous study was likely due to the duration of exposure- 9 d versus 4 d. In addition, lung toxicity was not examined at 1 d after exposure in the current PMET731 study. Like the current PMET731 study, the kinetics and magnitude of the lung response to the PMET720 thermal spray coating aerosol was quite different compared to the previous stainless steel welding fume inhalation study (Antonini et al. 2007). In addition, *in vitro* studies demonstrated that collected PMET720 particles were less cytotoxic to lung

macrophages compared to stainless steel welding particles, and their acellular reactivity and production of reactive oxygen species were several fold lower (Kodali et al. 2022).

The PMET540 wire was chosen for study as one of the most common acute health effects in workers exposed to Zn-containing fumes is metal fume fever (Wardhana and Datau 2014; Wong, Greene, and Robinson 2012). Metal fume fever is a self-limiting condition characterized by acute onset and flu-like symptoms that present within 48 hr and resolves in 1–2 d. Inhalation of aerosols generated using the Zn-based PMET540 wire in the current study had a significant but transient increase in both lung inflammation and injury at 4 d after exposure but returned to control levels by 30 d. The presence of neutrophils however were easily observed in the collected BAL cells after exposure to the Zn-based PMET540 aerosol at both time points. These findings were not surprising. In a previous study, a significant but transient increase in lung toxicity was observed in animals at 1 d after exposure (25 mg/m3 × 4 hr/d × 8 d) to a Zn-containing galvanized, spot welding fume (72.5% Fe, 26.3% Zn) that was similar in physical size and morphology to the PMET540 aerosol (Antonini et al. 2017). The lack of a persistent response in the current study was likely due to the rapid clearance of Zn from the lungs as nearly all (>98%) was cleared by 4 d post-exposure.

Unlike after exposure to the Zn-based PMET540 and stainless steel PMET731 aerosols, inhalation of the Ni-based PMET885 thermal spray coating aerosol caused significant loss in body weight compared to the air control during exposure, indicating an adverse effect on general health status of the animals. Even though these animals started to gain weight again after the exposure stopped, their body weight and the % change in body over time was significantly lower compared to air control at each time point. Importantly, lung injury and inflammation were significantly elevated at 4 d after exposure to the Ni-based PMET885 aerosol that persisted for 30 d. Lung inflammation was even more enhanced at 30 d after exposure compared to 4 d as total cells, AMs, and neutrophils were all significantly increased at the later time point. Interestingly, total cells were increased in the PMET885 group at 30 d post-exposure compared to 4 d. Cytospin micrographs showed that significant numbers of both neutrophils and EOS were clearly present in the recovered BAL cells at 4 and 30 d after exposure. Also, foamy macrophages and multinucleated giant cells were observed at the two times points after exposure to the Ni-based PMET885 aerosol. Foamy macrophages have a vacuolated cytoplasmic appearance that is characterized by an overaccumulation of phospholipids, proteins, and cellular debris (Lewis, Williams, and Beck 2014; Rossi et al. 2017). They are often present in cases of interstitial lung diseases and inflammation as was observed in the current study. Multinucleated giant cells also are observed in areas of lung inflammation and have been described as having a role in both disease progression and resolution (Miron and Bosshardt 2018).

In agreement with the results of the current study using the Ni-based PMET885 thermal spray coating aerosol, a Ni-based welding fume (containing minimal amounts of Cr) caused lung toxicity that persisted for up to 2 months after intratracheal instillation exposure that was not observed with a mild steel and stainless steel welding fume (Antonini et al. 2014). Assessing phagocytic cell cytotoxicity, the Ni-based welding fume in the same study caused significant loss of lung macrophage viability at a lower dose (50 μg/ml) in comparison to

the mild steel and stainless steel welding fume samples, suggesting the Ni-based welding fume was more cytotoxic than the other two welding fumes. This elevated cytotoxic effect of the Ni–based welding fume was likely due to the amount of Ni present, as Ni-containing particles have been shown to be toxic to lung epithelial cells (Volke et al. 2013) and lung macrophages (Antonini et al. 2003). It is important to note that this finding may not be explained by Ni amount only, as the stainless steel fume had a similar amount of Ni present. The Ni–based welding fume contained significant amounts of Cu, Ti, and Al that were not present in the other welding fume samples.

To compare the pulmonary clearance of deposited metals after inhalation of the different thermal spray coating aerosols in the current study, the concentrations of individual metals were measured in the lungs at different time points after a single exposure (25 mg/m^3 × 4 h/d × 1d) to the different thermal spray coating aerosols. Because the lung tissue concentrations in the control animals were not trivial for some metals and may complicate the assessment of clearance, the values for the specific metals (Ni, Zn, Cr, Fe, and Mn) of the air control samples were subtracted from the corresponding metal concentrations measured in the lungs after exposure to the different thermal spray aerosols. For the PMET885 aerosol, the Ni concentrations in the control lungs were <1% of the values in the exposed animals. The clearance pattern did not appear to be reflected by a single exponential (i.e. one-compartment model) but appeared to indicate an initial fast clearance followed by a slower rate. This could reflect a combination of dissolution and particle transport (phagocyte and mucociliary clearance). For the PMET540 aerosol, the Zn concentrations in the exposed animals were only significantly greater than those for the control animals at 0 and 1 d. These values showed extremely fast clearance, and a reasonable hypothesis was rapid dissolution of the deposited metal particles and clearance. For the stainless steel PMET731 aerosol, the assessment of lung burden was more complex. The concentrations of Fe in the exposed animals were only significantly greater than the control values at 0 and 1 d. Also, the Fe value at 1 d was higher than that at 0 d, possibly reflecting a wide range in the control values, making it difficult to assess lung clearance on the basis of the Fe value. The clearance of Cr and Mn concentrations were clearer as the control levels for both were negligible. They had similar rates of clearance as nearly half of the deposited Cr and Mn were cleared by 4 d. A small but significant percentage of each of these metals (Cr: 23.2%; Mn 11.8%) persisted in the lungs at 30 d after exposure.

Ongoing studies are evaluating multiple *in vitro* toxicity and functional screening assays using different Ni-based thermal spray coating particles to assess the possible cellular and molecular mechanisms involved in the whole animal lung responses. The mechanisms being studied include phagocytic cell cytotoxicity and activation, changes in intracellular oxidative stress, and alterations in cellular uptake of particles. Also, because of the exaggerated lung response to the Ni-based PMET885 aerosol, additional inhalation toxicology studies are being performed using three different exposure concentrations and multiple Ni-based thermal spray aerosols generated from different wires with varying Ni compositions as well as evaluating possible long-term lung pathology at longer post-exposure time points (e.g. 90, 120 d) after exposure.

5. Conclusions

A thermal spray coating generator and inhalation exposure system has been developed to perform animal studies to mimic workplace exposures. The generated particles were arranged as chain-like agglomerates and had similar MMAD (310–378 nm). Inhalation of PMET885 aerosol caused a significant increase in lung in jury and inflammation at both time points examined. Inhalation of PMET540 aerosol caused only a slight but transient increase in lung toxicity, whereas exposure to the PMET731 aerosol had no effect on the lung responses at either time point. The deposited metals after exposure to PMET885 and PMET731 aerosols had similar clearance kinetics. The deposited Zn for the PMET540 aerosol was cleared much more quickly compared to the other test aerosols. Comparison of thermal spray coating aerosols indicated that varied lung responses (e.g. PMET885 >> PMET540 ≥ PMET731) and clearance kinetics are dependent on the consumables used.

The completion of this project will provide new information on exposures and health effects of thermal spray coating and possibly lead to intervention of any potential occupational health hazards as the industry develops. The current study was designed to facilitate initial field and ongoing worker health studies by identification, characterization, and toxicological assessment of the potentially hazardous aerosols in a laboratory setting. The results from the current project will be disseminated and translated to industries involved in thermal spray coating. In addition, dose-response and time-course information about thermal spray coating aerosols will be generated for risk assessment analysis.

Funding

This work was supported by the National Occupational Research Agenda of the National Institute for Occupational Safety and Health project #93909NE.

Data availability statement

Data included in the current manuscript will be made available to the public after the acceptance of publication.

References

Afshari AA, McKinney W, Cumpston JL, Leonard HD, Cumpston JB, Meighan TG, Jackson M, et al. 2022. "Development of a Thermal Spray Coating Aerosol Generator and Inhalation Exposure System." Toxicology Reports 9: 126–135. 10.1016/j.toxrep.2022.01.004 [PubMed: 35127456]

Antonini JM, McKinney WG, Lee EG, and Afshari AA. 2021. "Review of the Physicochemical Properties and Associated Health Effects of Aerosols Generated during Thermal Spray Coating Processes." Toxicology and Industrial Health 37 (1): 47–58. 10.1177/0748233720977975 [PubMed: 33305691]

Antonini JM, Kodali V, Shoeb M, Kashon M, Roach K, Boyce G, Meighan T, et al. 2020. "Effect of a High Fat Diet and Occupational Exposure in Different Rat Strains on Lung and Systemic

Responses: Examination of the Exposome in an Animal Model." Toxicological Sciences 174 (1): 100–111. 10.1093/toxsci/kfz247 [PubMed: 31868906]

Antonini JM, Afshari A, Meighan TG, McKinney W, Jackson M, Schwegler-Berry D, Burns DA, et al. 2017. "Aerosol Characterization and Pulmonary Responses in Rats after Short-Term Inhalation of Fumes Generated during Resistance Spot Welding of Galvanized Steel." Toxicology Reports 4: 123–133. 10.1016/j.toxrep.2017.02.004 [PubMed: 28959633]

Antonini JM, Badding MA, Meighan TG, Keane MK, Leonard SS, and Roberts JR. 2014. "Evaluation of the Pulmonary Toxicity of a Fume Generated from a Nickel-, Copper-Based Electrode to Be Used as a Substitute in Stainless Steel Welding." Environ Health Insights 8 (Suppl 1): 11–20. [PubMed: 25392698]

Antonini JM, Stone S, Roberts JR, Chen B, Schwegler-Berry D, Afshari AA, and Frazer DG. 2007. "Effect of Short-Term Stainless Steel Welding Fume Inhalation Exposure on Lung Inflammation, Injury, and Defense Responses in Rats." Toxicology and Applied Pharmacology 223 (3): 234–245. 10.1016/j.taap.2007.06.020 [PubMed: 17706736]

Antonini JM, Taylor MD, Zimmer AT, and Roberts JR. 2003. "Pulmonary Responses to Welding Fumes: Role of Metal Constituents." Journal of Toxicology and Environmental? 67 (3): 233–249. 10.1080/15287390490266909

ASM Thermal Spray Society. 2023. Thermal spray Technology White Paper. Accessed September 20, 2023. http://www.asminternational.org/web/tss/technical/white-paper.

Bahl A, Hellack B, Wiemann M, Giusti A, Werle K, Haase A, and Wohlleben W. 2020. "Nanomaterial Categorization by Surface Reactivity: A Case Study Comparing 35 Materials with Four Different Test Methods." NanoImpact 19: 100234. 10.1016/j.impact.2020.100234

Bémer D, Régnier R, Subra I, Sutter B, Lecler MT, and Morele Y. 2010. "Ultrafine Particles Emitted by Flame and Electric Arc Guns for Thermal Spraying of Metals." The Annals of Occupational Hygiene 54 (6): 607–614. 10.1093/annhyg/meq052 [PubMed: 20685717]

Chadwick J, Wilson H, and White M. 1997. "An Investigation of Occupational Metal Exposure in Thermal Spraying Processes." The Science of the Total Environment 199 (1–2): 115–124. 10.1016/s0048-9697(97)05487-9 [PubMed: 9200854]

Darut G, Dieu S, Schnuriger B, Vignes A, Morgeneyer M, Lezzier F, Devestel F, et al. 2021. "State of the Art of Particle Emissions in Thermal Spraying and Other High Energy Processes Based on Metal Powders." Journal of Cleaner Production 303: 126952. 10.1016/j.jclepro.2021.126952

Grand View Research. 2023. Thermal Spray Coatings Market Worth $15.41 Billion by 2030. Accessed June 20, 2023. https://www.grandviewresearch.com/press-release/global-thermal-spray-coating-market.

Huang H, Li H, and Li X. 2016. "Physicochemical Characteristics of Dust Particles in HVOF Spray and Occupational Hazards: Case Study in a Chinese Company." Journal of Thermal Spray Technology 25 (5): 971–981. 10.1007/s11666-016-0422-8

Kodali V, Afshari A, Meighan T, McKinney W, Mazumder MHH, Majumder N, Cumpston JL, et al. 2022. "*In Vivo* and *In Vitro* Toxicity of a Stainless-Steel Aerosol Generated during Thermal Spray Coating Using an Animal Inhalation Model." Archives of Toxicology 96 (12): 3201–3217. 10.1007/s00204-022-03362-7 [PubMed: 35984461]

Leonard SS, Roberts JR, Antonini JM, Castranova V, and Shi X. 2004. "PbCrO 4 Mediates Cellular Responses via Reactive Oxygen Species." Molecular and Cellular Biochemistry 255 (1–2): 171–179. 10.1023/b:mcbi.0000007273.23747.67 [PubMed: 14971658]

Lewis DJ, Williams TC, and Beck SL. 2014. "Foamy Macrophage Responses in the Rat Lung following Exposure to Inhaled Pharmaceuticals: A Simple, Pragmatic Approach for Inhaled Drug Development." Journal of Applied Toxicology 34 (4): 319–331. 10.1002/jat.2950 [PubMed: 24474237]

Miron RJ, and Bosshardt DD. 2018. "Multinucleated Giant Cells: Good Guys or Bad Guys?" Tissue Engineering. Part B, Reviews 24 (1): 53–65. 10.1089/ten.TEB.2017.0242 [PubMed: 28825357]

NIOSH. 2018. "Elements in Tissues: Method 8200." In NIOSH Manual of Analytical Methods, 5th ed., Cincinnati, OH: U.S. Department of Health and Human Services. DHHS Publication No. 2014–2151.

Metco Oerlikon. 2016. "An Introduction to Thermal Spray." Issue 6.

An Introduction to Thermal Spray – Microsofte¦ An Introduction to Thermal Spray – Issue 6 – July 2016 10 2.4.4 High Velocity Oxy-Fuel Spray (HVOF) The high velocity oxy-fuel – [PDF Document] (fdocuments.net) (Accessed September 20, 2023).

Petsas N, Kouzilos G, Papapanos G, Vardavoulias M, and Moutsatsou A. 2007. "Worker Exposure Monitoring of Suspended Particles in a Thermal Spray Industry." Journal of Thermal Spray Technology 16 (2): 214–219. 10.1007/s11666-007-9027-6

Rossi G, Cavazza A, Spagnolo P, Bellafiore S, Kuhn E, Carassai P, Caramanico L, et al. 2017. "The Role of Macrophages in Interstitial Lung Diseases." European Respiratory Review 26 (145): 170009. 10.1183/16000617.0009-2017 [PubMed: 28724562]

Salmatonidis A, Ribalta C, Sanfelix V, Bezantakos S, Biskos G, Vulpoi A, Simion S, Monfort E, and Viana M. 2019. "Workplace Exposure to Nanoparticles during Thermal Spraying of Ceramic Coatings." Annals of Work Exposures and Health 63 (1): 91–106. 10.1093/annweh/wxy094 [PubMed: 30551164]

Stefaniak AB, Harvey CJ, Bukowski VC, and Leonard SS. 2009. "Comparison of Free Radical Generation by Pre-and Post-Sintered Cemented Carbide Particles." Journal of Occupational and Environmental Hygiene 7 (1): 23–34. 10.1080/15459620903349073

U.S. Bureau of Labor Statistics. 2022. Occupational Employment and Wages, 51–9124 Coating, painting, and spraying machine setters, operators, and tenders." Coating, Painting, and Spraying Machine Setters, Operators, and Tenders (bls.gov) (Accessed 09/20/2023).

Volke A, Rünkorg K, Wegener G, Vasar E, and Volke V. 2013. "Dual Effect of Nickel on L-Arginine/Nitric Oxide System in RAW 264.7 Macrophages." International Immunopharmacology 15 (3): 511–516. 10.1016/j.intimp.2013.01.019 [PubMed: 23415871]

Wardhana E and Datau A. 2014. "Metal Fume Fever among Galvanized Welders." Acta Medica Indonesiana 46: 256–262. [PubMed: 25348190]

Wong A, Greene S, and Robinson J. 2012. "Metal Fume Fever: A Case Review of Calls Made to the Victorian Poisons Information Center." Aust Fam Physician 41: 141–144. [PubMed: 22396928]

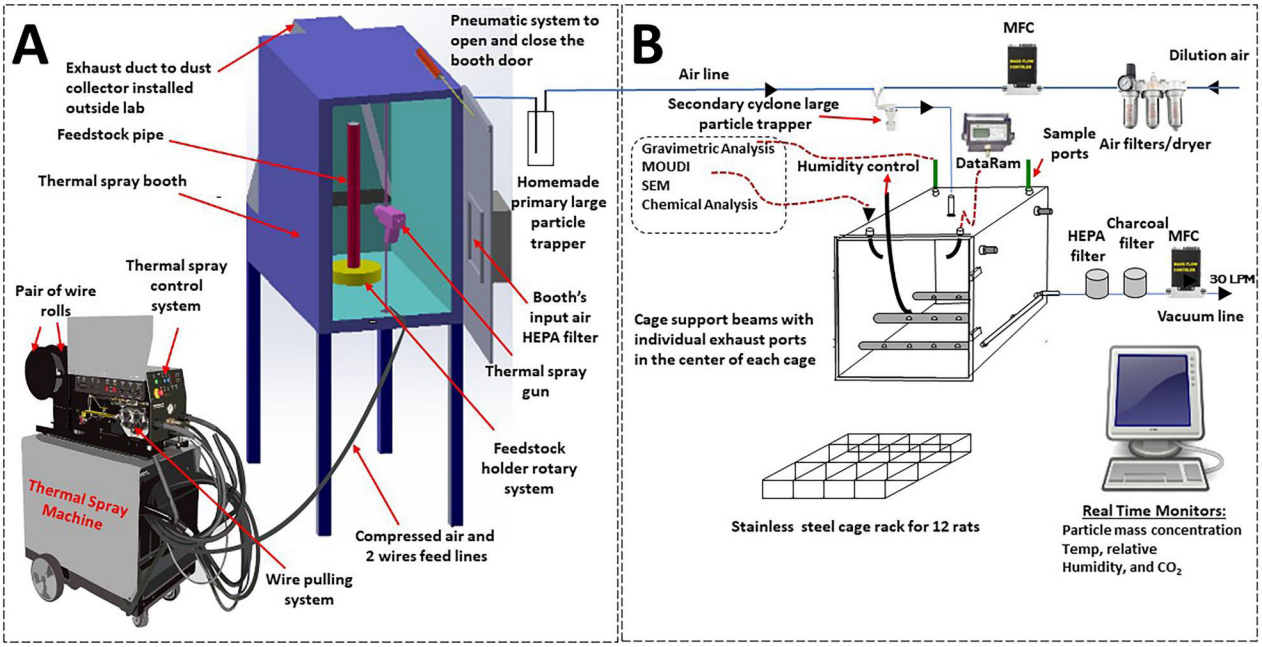

Figure 1.

Diagram of the NIOSH electric arc wire thermal spray coating aerosol generator and exposure system (modified from Afshari et al., 2022). Thermal spray coating was performed in one room (a), and the aerosols piped to an exposure chamber in a separate room (B) divided by shaded glass doors and protective curtain. Abbreviations: Data Ram = real-time aerosol monitor; MOUDI = Micro Orifice Uniform Deposit Impactor; SEM = scanning electron microscopy; Temp = temperature; LPM = liters per minute; MFC = mass flow controller.

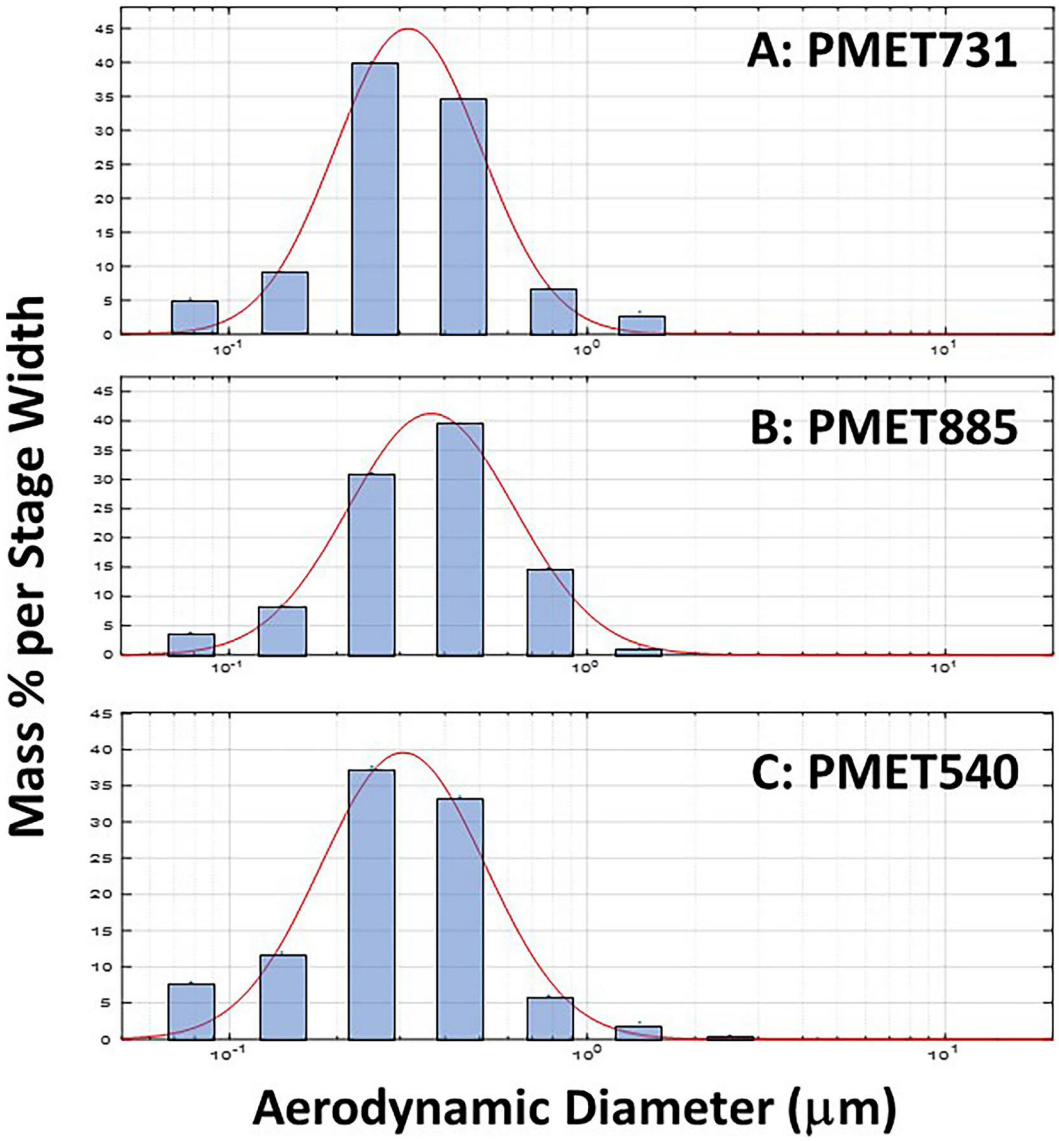

Figure 2.

Representative particle size distribution graphs of generated during electric arc thermal spray coating using the following consumable wires: (A) PMET731; (B) PMET885; (C) PMET540. The mass percent per stage width versus aerodynamic diameter was compared as measured by a MOUDI particle impactor. The mass percent per stage width is the percentage of total mass of particles deposited on each stage of the MOUDI impactor normalized by the width of each stage.

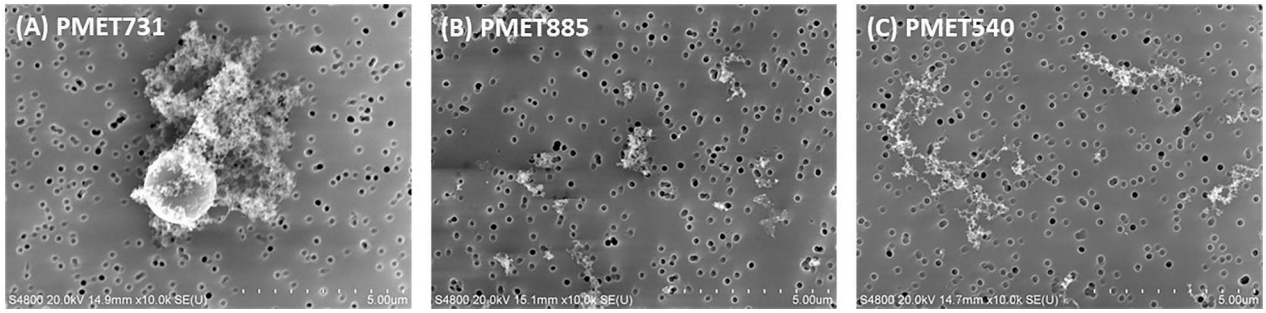

Figure 3.

Representative SEM images of particles generated during electric arc thermal spray coating using the following consumable wires: (A) PMET731; (B) PMET885; (C) PMET540. Scale bar (represented by the white dashed line) = 5 μm.

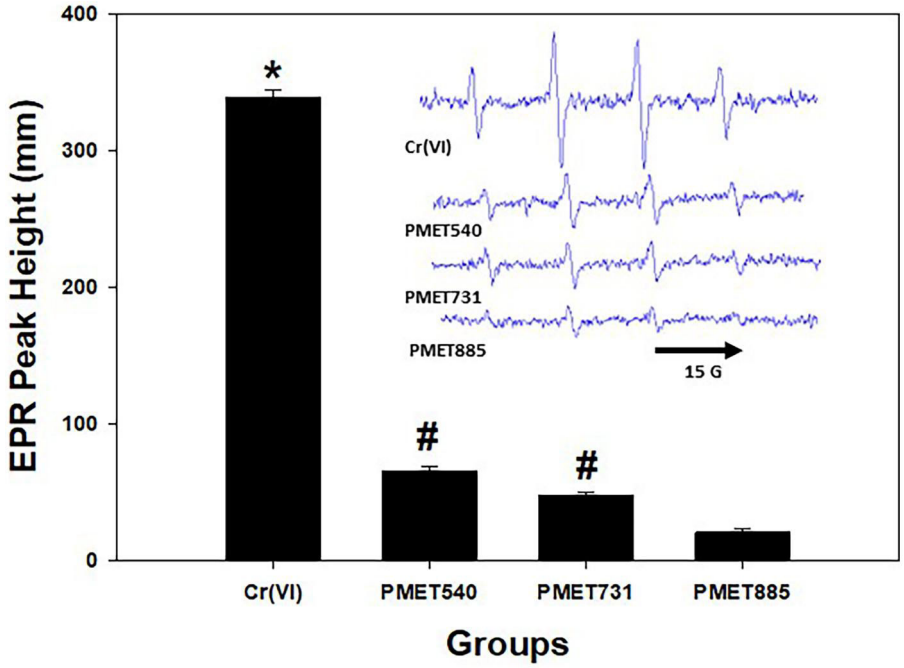

Figure 4.

EPR peak height and spectra (inset) with PMET731, PMET885, and PMET540 collected thermal coating particle samples and positive control [2 mM Cr (VI)]. Data (n= 3/group) are means ± standard error; significantly different from all groups; [#]Significantly different from the PMET885 group ($p < 0.05$).

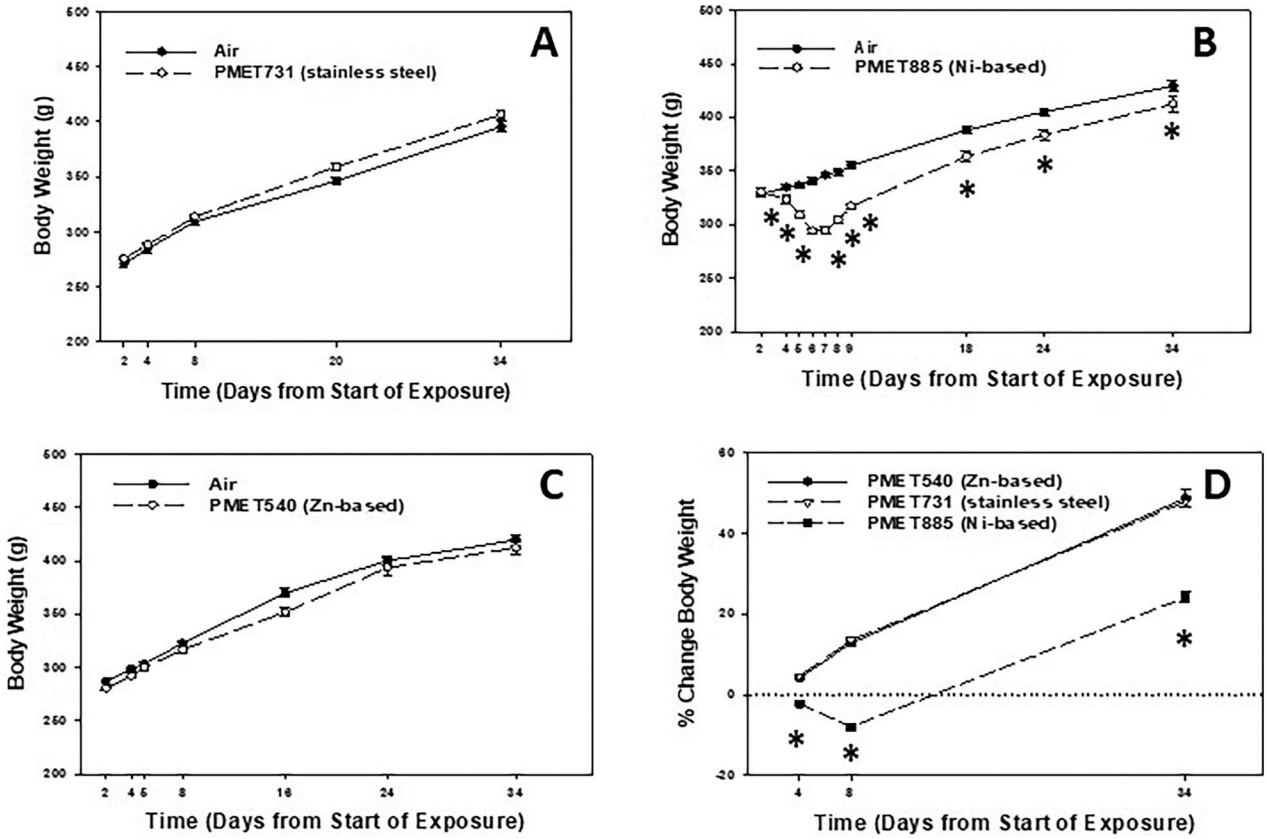

Figure 5.

Body weight of animals after inhalation exposure to (A) PMET731, (B) PMET885, and (C) PMET540. (D) % change in body weight of animals after exposure to the different thermal spray coating aerosols. Male Sprague-Dawley rats were exposed to a target concentration of 25 mg/m^3 × 4 hr/d × 4 d (n= 12 rats/treatment group up to 8 days; n= 6 rats/treatment group after 8 days). *Significantly different from corresponding air control within a time point (p < 0.05).

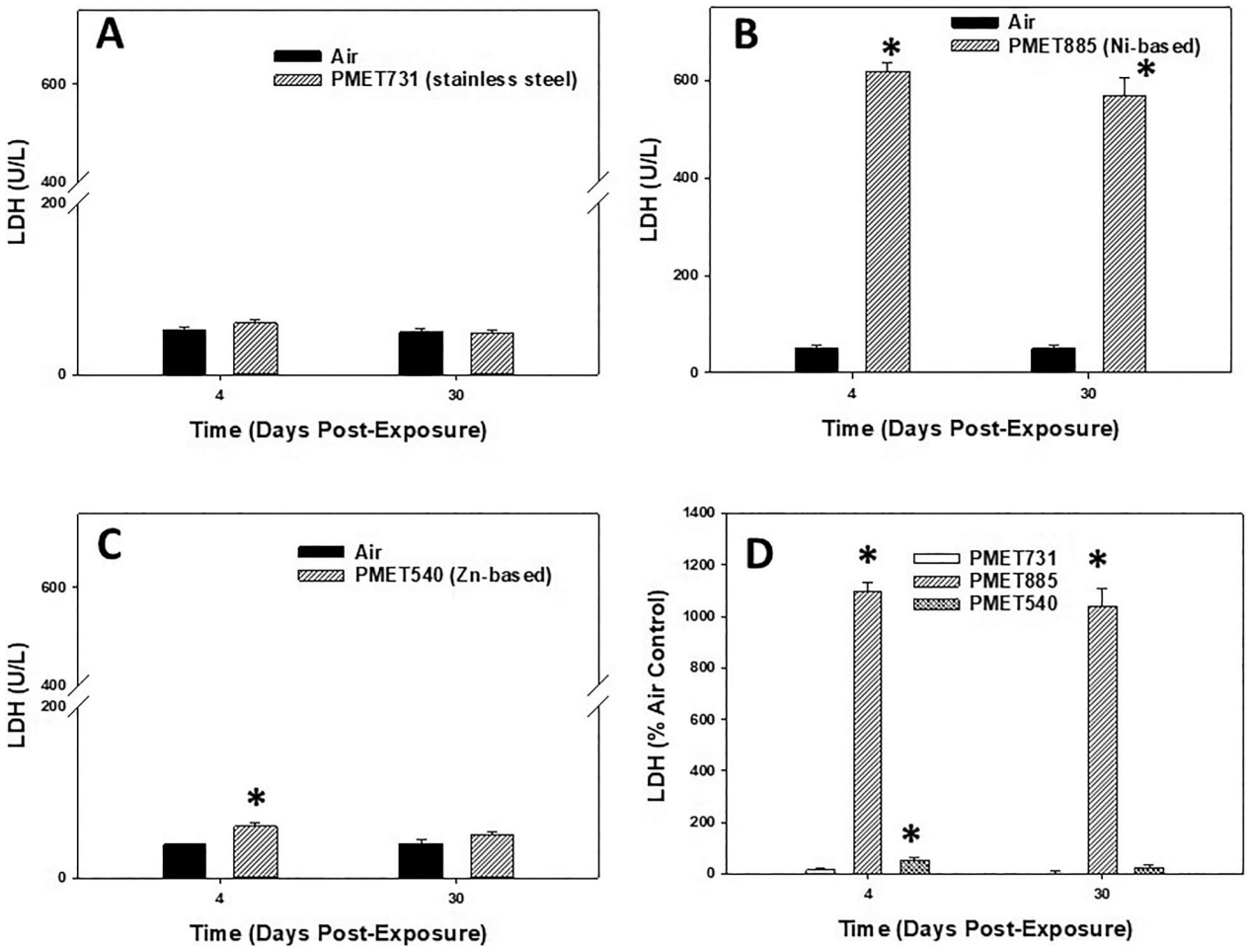

Figure 6.

BALF LDH at 4 and 30 d after inhalation exposure to (A) PMET731, (B) PMET885, (C) PMET540, and (D) % air control of LDH for each different thermal spray coating aerosol. Male Sprague-Dawley rats (n= 6/treatment group within a time point) were exposed to a target concentration of 25 mg/m^3 × 4 hr/d 4 × d. *Significantly different from corresponding air control within a time point ($p < 0.05$).

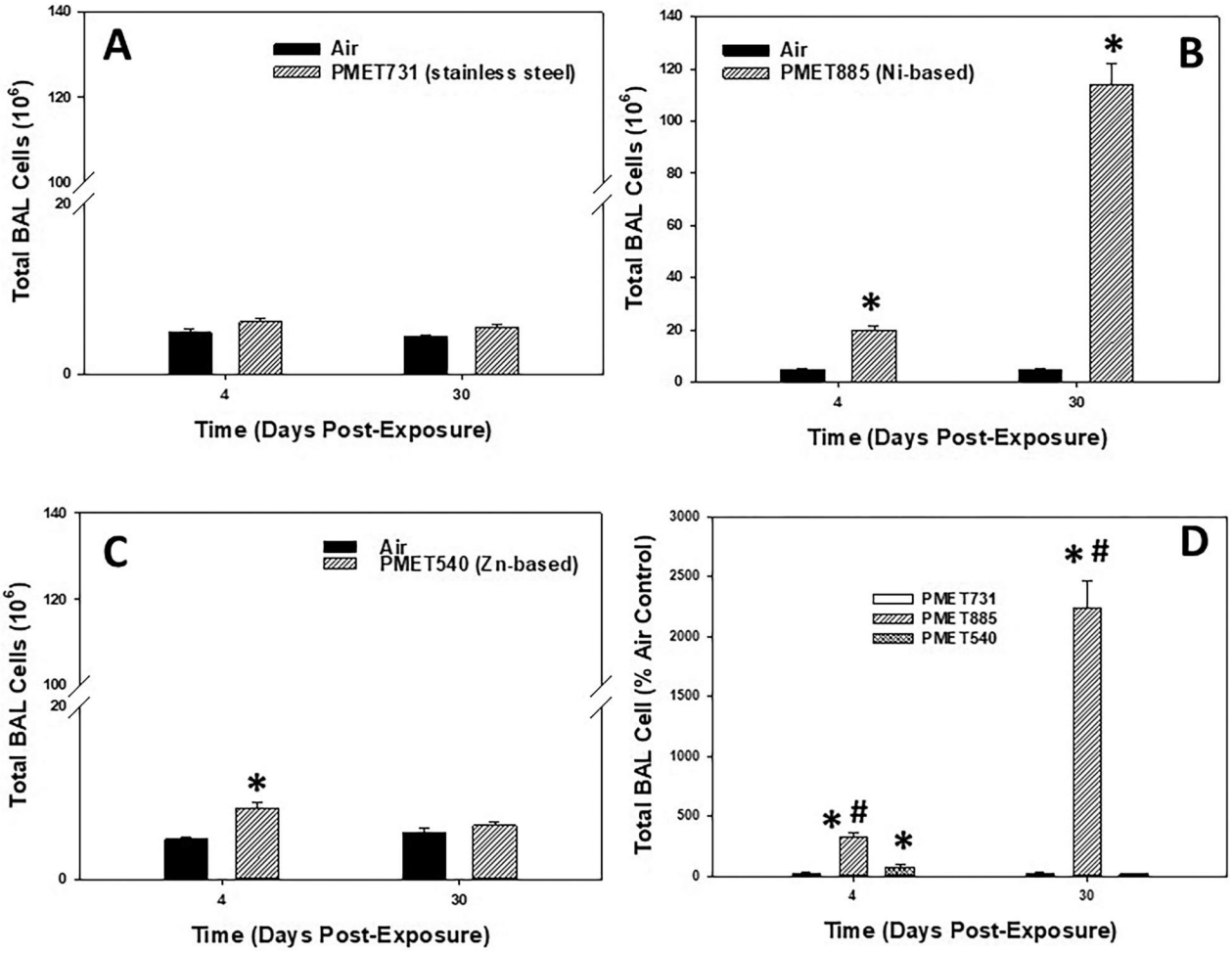

Figure 7.

Total BAL cells at 4 and 30 d after inhalation exposure to (A) PMET731, (B) PMET885, and (C) PMET540, and (D) % air control of total BAL cells for each different thermal spray coating aerosol. Male Sprague-Dawley rats (n= 6/treatment group within a time point) were exposed to a target concentration of 25 mg/m^3 × 4 hr/d 4 × d. *significantly different from corresponding air control within a time point; $^{\#}$significantly different from other groups within a time point ($p < 0.05$).

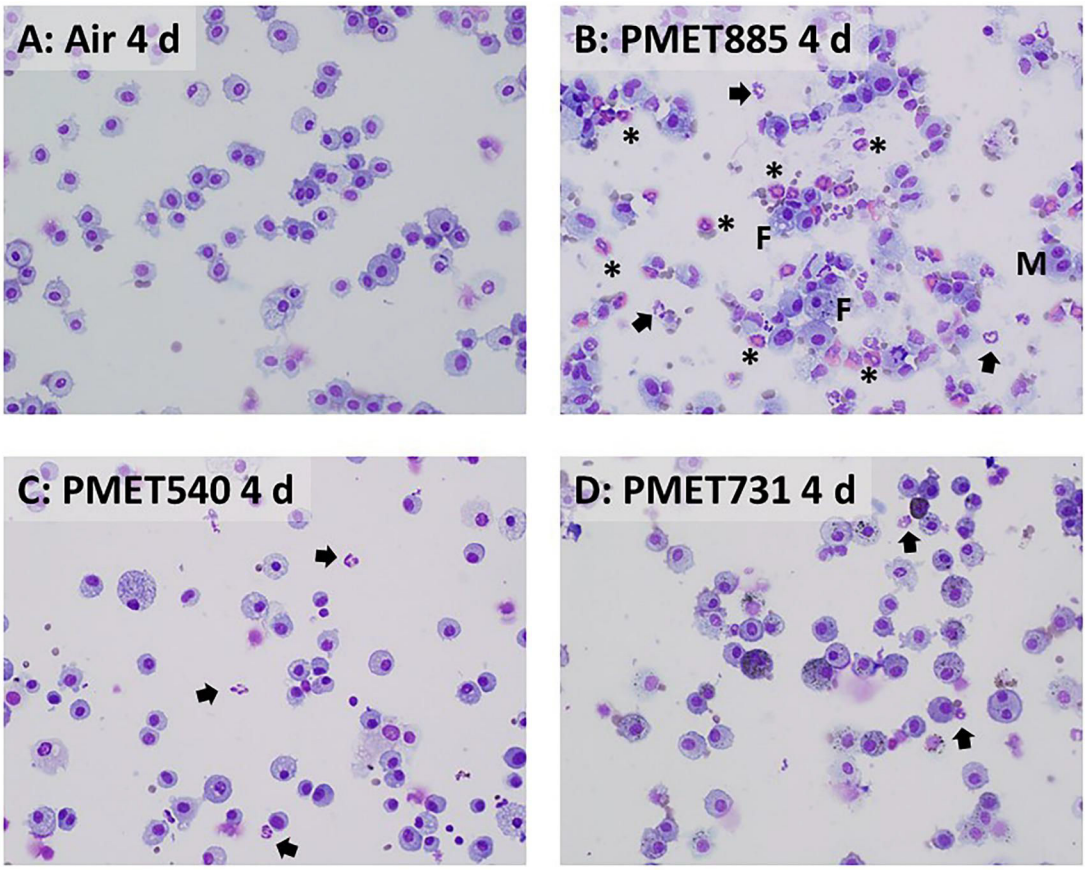

Figure 8.

Representative cytospin photomicrographs of recovered BAL cells at 4 d after exposure to air (A; control) or 25 mg/m^3 of (B) PMET885, (C) PMET540, and (D) PMET731 thermal spray coating aerosols. Arrows = neutrophils; asterisks = eosinophils; M = multinucleated giant cells; F = foamy cells. Magnification is 40x.

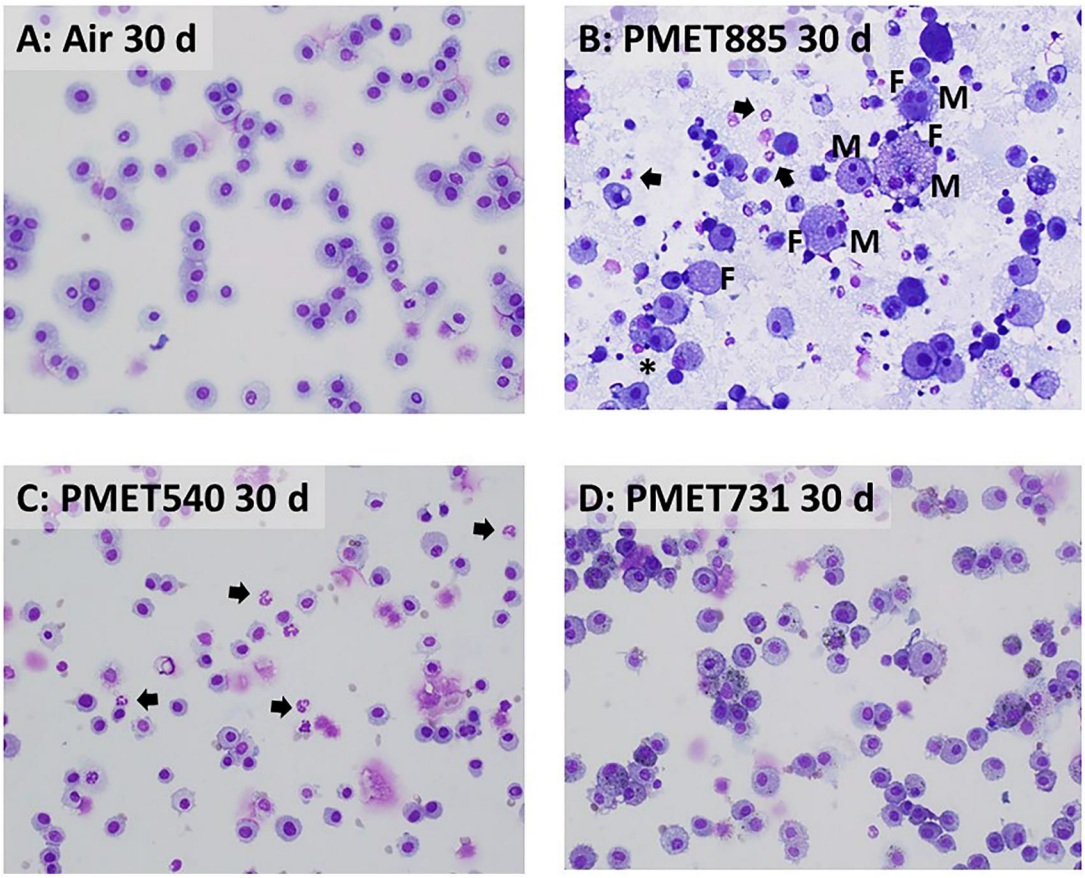

Figure 9.

Representative cytospin photomicrographs of recovered BAL cells at 30 d after exposure to air (A; control) or 25 mg/m^3 of (B) PMET885, (C) PMET540, and (D) PMET731 thermal spray coating aerosols. Arrows = neutrophils; asterisks = eosinophils; M = multinucleated giant cells; F = foamy cells. Magnification is 40x.

Table 1.

Thermal spray coating particle composition and size.

Wire Type	Metal Composition (weight %)[a]	MMAD (nm)	Geometric Standard Deviation
PMET731: stainless steel	Fe 66.3±0.56	310	1.94
	Cr 26.2±0.57		
	Mn 1.02±0.02		
PMET885: Ni-based	Ni 96.9±0.63	316	1.94
	Al 1.69±0.03		
	Zn 1.06±0.32		
	Fe 0.699±0.11		
PMET540: Zn-based	Zn 99.4±0.24	378	1.89
	Ni 0.325±0.16		
	Fe 0.235±0.14		

[a]Relative to all metals analyzed; Values are means± standard error (n=4); portions of this data were modified from Afshari et al. (2022).

Table 2.

BAL cell differential after exposure to PMET731, PMET885, and PMET540 thermal spray coating aerosols.

Treatment Groups	Time (Days Post-Exposure)	BAL Alveolar Macrophages (106)	BAL Neutrophils (106)	BAL Eosinophils (106)
Air PMET731	Day 4	4.87±0.41	0.008±0.008	0.00±0.00
		5.68±0.27	0.46±0.12	0.00±0.00
Air PMET731	Day 30	4.38±0.20	0.008+0.005	0.00±0.00
		5.07±0.53	0.38±0.12	0.00±0.00
Air PMET885	Day 4	4.68±0.52	0.020±0.001	0.03±0.02
		12.7±1.9*	4.15±0.43*	2.29±0.74*
Air PMET885	Day 30	4.42±0.28	0.128±0.12	0.00±0.00
		91.1±8.3*	18.5±3.8*	3.07±1.06*
Air PMET540	Day 4	4.61±0.17	0.005±0.005	0.00±0.00
		7.81+0.60*	0.33±0.08	0.010+0.01
Air PMET540	Day 30	5.36±0.50	0.008±0.003	0.00±0.00
		6.19 ±0.46	0.030±0.010	0.020±0.02

Note. Male Sprague-Dawley rats (*n*=6/treatment group within a time point) were exposed to a target concentration of 25mg/m^3 × 4hr/d × 4 d. For BAL cell differential analysis, 200 cells/rat were counted.

*Significantly different from corresponding air control within a time point ($p<0.05$).

Table 3.

Lung concentration of specific metals after exposure to PMET731, PMET885, and PMET540 thermal spray coating aerosols.

Metal (time post-exposure)	Control (μg/g dry lung tissue)	Thermal Spray Coating (μg/g dry lung tissue)	Thermal Spray Coating minus Air Control (% metal remaining in lungs)
Ni	Air	PMET885	Ni - Air
0 d	0.271±0.06	168±10 *	168
1 d	0.227±0.05	166±12 *	166 (98.8%)
4 d	0.230 + 0.05	89.5±1.2 *	89.3 (53.2%)
30 d	0.290±0.03	35.9±1.6 *	35.6 (21.2%)
Zn	Air	PMET540	Zn - Air
0 d	88.0±4.9	161±4.6 *	73
1 d	85.2±2.1	104±6.4 *	18.8 (25.8%)
4 d	87.9±2.2	83.3±1.7	−4.6 (−6.30%)
30 d	79.8±2.4	74.2±3.1	−5.6 (−7.67%)
Cr	Air	PMET731	Cr - Air
0 d	n.d.	48.7±2.7 *	48.7
1 d	n.d.	48.6±1.8 *	48.6 (99.8%)
4 d	n.d.	26.3±2.5 *	26.3 (54.0%)
30 d	n.d.	11.3±1.7 *	11.3 (23.2%)
Fe			Fe - Air
0 d	315±13	463±25 *	148
1 d	326±11	522±26 *	196 (132%)
4 d	357±20	378±23	21 (14.2%)
30 d	392±9.5	423±25	31 (20.9%)
Mn			Mn - Air
0 d	0.800±0.04	2.67±0.11 *	1.87
1 d	0.780±0.02	2.33±0.07 *	1.55 (82.8%)
4 d	0.810±0.01	1.74±0.08 *	0.93 (49.7%)
30 d	0.840±0.08	1.06±0.04 *	0.22 (11.8%)

Note. Male Sprague-Dawley rats (n=6/treatment group within a time point) were exposed to a target concentration of 25mg/m^3 × 4hr/d × 4 d.

* Specific metal is significantly different from corresponding air control within a time point (p<0.05). n.d. = below level of quantification.